

Sensor and Control Concept for a Wearable Robot for Manual Load Handling Assistance

Patrick Stelzer¹, Bernward Otten², Werner Kraus¹ and Andreas Pott¹

¹*Fraunhofer Institute for Manufacturing Engineering and Automation (IPA), Stuttgart, Germany, e-mail: patrick.stelzer@ipa.fraunhofer.de*

²*Helmut Schmidt University, Hamburg, Germany, e-mail: ben.otten@hsu-hh.de*

Abstract. Current wearable robots mostly focus on applications in military, rehabilitation and load lifting in the health sector, while they are hardly used in industry and manufacturing. In this paper, a sensor and control concept for a wearable robot for assistance in manual handling of loads in industry is presented. Special requirements such as low costs, direct contact between the human and the load and easy set-up are addressed. A wall-mounted test stand of an actuated elbow joint was built up to evaluate the proposed sensors and control algorithms. By using a torque sensor in the elbow joint as reference it is shown that low cost force sensors in the forearm can be used to measure the human-robot interaction. A torque-based and a velocity-based impedance control approach are compared which allow the user to move freely while not handling any loads and which also allow to incorporate a human command signal for regulation of force support. The former is shown to be superior to the position-based approach. Further, the influence of the human impedance characteristics onto stability of the controllers is discussed.

Key words: Wearable Robots, Exoskeletons, Impedance Control, Resistive Sensors, Manual Load Handling.

1 Introduction

Manual handling of loads (MHL) is a common task for workers in industry, especially in the sector of logistics and transport. According to the European Agency for Safety and Health at Work, MHL is one of the major causes for musculoskeletal disorders (MSD), which are the most serious health problem affecting European workers, more than 50 percent reported to suffer from MSD [17].

Current assistance systems focus on avoiding MHL, examples are cranes, rope balancers or fork lifts. However, most MHL tasks are characterized by an immense diversity of load weights, sizes, shapes and environmental conditions at the workplace and therefore require the flexibility and cognition of human workers. To combine the physical strength of the robot with human's flexibility and cognitive capabilities, assistance systems can be attached directly to the worker. Such systems, referred to as exoskeletons or wearable robots, could then reduce work related injuries and increase productivity by reducing the strain on the musculoskeletal system and

maintaining the workers performance constant over a full working day. However, industrial applications have special requirements regarding the sensor and control concept. For acceptance of the system by the worker an easy set up is required, that is a complicated or time-consuming sensor placement is not acceptable. The control of the system must be possible in an intuitive way such that the worker is not impeded in his handling task, which in general requires both hands. The used sensors must be reliable, cost-effective and lightweight.

In the last decades numerous research on wearable robots was done, however, mostly for applications in rehabilitation, military and load lifting in the health sector, e.g. [4, 5, 15]. For example, the *muscle suit* from Tokyo University [11] is an upper limb exoskeleton for load lifting in the health sector with pneumatic actuators for the elbow, shoulder and hip joint. The system produces a static support force and no detection of user intention is done. Other exoskeletons detect the user intention by using sensors based on electromyography (EMG) or force [18, 6, 12, 3]. However, EMG based sensors are known to be unreliable and strongly user-dependent, see e.g. [7], and they have to be attached to the human skin which makes them not suitable for the given application. Force sensors, on the other hand, are more reliable and easy to integrate, however, mostly multiaxial force cells are used which are costly, relatively big and heavy. Recently, the company Innophys announced to produce an upper limb exoskeleton based on the *muscle suit* which can be controlled by the user via an air tube in the mouth, which is not feasible for long operation times.

Regarding control, current exoskeletons mostly use impedance control which is suitable for use in contact tasks [21]. Commonly two implementations of impedance control exist, originally presented as force-based impedance control and position-based impedance control [13], in the following both approaches will be referred to as impedance and admittance control, respectively. Their differences will be discussed below.

In this paper, a control and sensor concept for an exoskeleton for assistance of workers in MHL tasks in industry is presented. The exoskeleton is not supposed to fully compensate load weights or to augment the human wearer's force capabilities, but to reduce the necessary force input by the user and hence maintain performance and health. In contrast to existing systems our concept is based on cost-effective and lightweight force sensors in the front cuff of the forearm brace which can generate a passive movement of the elbow joint according to the worker's intention. An impedance controller is shown to perform better than an admittance controller and stability issues of the control concept are discussed. The control concept allows to incorporate a human control signal for active force support. For this purpose we propose an intelligent sensor glove (see [19] and [14]), which is outside the scope of this paper. Hence, the worker does not need to grip a handle or a remote control. For evaluation of the concept a wall-mounted test stand with an actuated elbow joint and a three degree of freedom (dof) shoulder kinematics was built up, see Fig. 1. The actuator is placed directly on the elbow joint to ensure good control performance. The exoskeleton arm is attached to the user via an arm brace at the forearm, consisting of a front and a back cuff. The front cuff comprises a revolute joint allowing pronation and supination of the forearm. Note that this arm exoskeleton is not meant

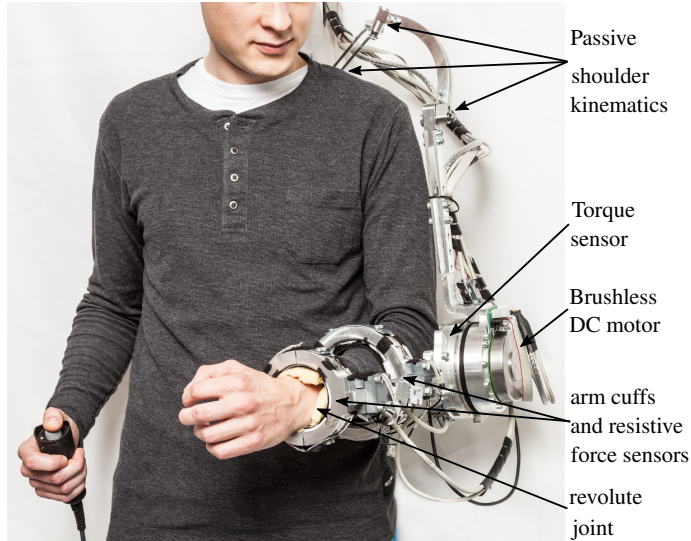


Fig. 1 Wall-mounted test stand of the left arm kinematics with actuated elbow joint, 3-dof shoulder kinematics and forearm brace

to be wearable, it is used to evaluate the control and sensor concept under constant and repeatable conditions. A body-worn version will be constructed based on the findings of this paper. In Fig. 2 the schematic structure of the system is shown.

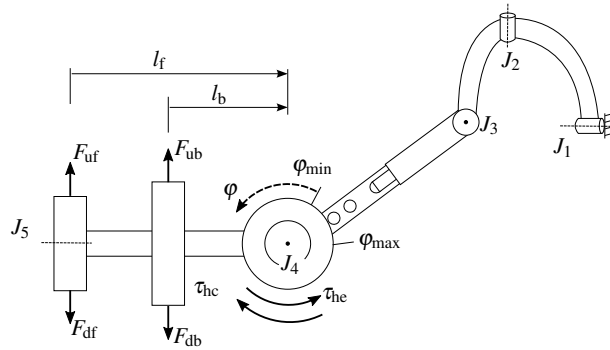


Fig. 2 Schematic structure of the wall-mounted test stand

The paper is organized as follows: In Section 2 the sensor concept for detection of the user intention is presented and verified in measurements, Section 3 presents the proposed control algorithms. In Section 4 the experimental set-up is described and the proposed controllers are evaluated. Section 5 summarizes the results and gives an outlook.

2 Sensor Concept

In MHL tasks the user needs to grip a load using his hands, i.e. direct contact between the user and the load is necessary such that the load directly acts on the human hand, not on the exoskeleton construction. In this case force-based sensors at the human-exoskeleton attachment point(s) can only be used to produce a passive movement rather than generate active force support. For this reason, the exoskeleton is supposed to be operated in two different modes. In case the wearer wants to move freely, i.e. if no physical support is required, the exoskeleton must passively follow the wearer's movements and provide full flexibility. This operation mode is referred to as an idle-mode. The second mode, referred to as force-support mode, is given if the user is manually handling loads and needs physical support, i.e. the system must provide force support. In both operating modes the intention of the user needs to be detected. In case of the idle-mode the relevant interaction forces and torques between the user and the exoskeleton can be determined and then transferred to an appropriate movement of the actuated joints. For this purpose, the actuated joints can be equipped with an one-axis torque sensor each. However, to reduce cost and weight, thin-like force sensors in the cuffs of the forearm brace are proposed to replace the torque sensor in the elbow joint. In theory four force sensors, two in each cuff, are necessary to calculate the human-exoskeleton interaction torque τ_{he} around J_4 as

$$\tau_{\text{he}} = (F_{\text{df}} - F_{\text{uf}}) l_f + (F_{\text{db}} - F_{\text{ub}}) l_b \quad , \quad (1)$$

with measured forces in the arm cuffs $F_{\text{df}}, F_{\text{uf}}, F_{\text{db}}, F_{\text{ub}}$ and positions of the arm cuffs $l_f = 260$ mm and $l_b = 114$ mm, according to Fig. 2. We propose to use the two sensors in the front cuff only which dominate the measurement as $l_f > l_b$, i.e. reducing the necessary number of sensors by half and reducing the weight of the forearm brace, as the back cuff can be designed much more compact if it does not carry any sensors.

To evaluate this concept the elbow joint was fixed in three different angular positions, an upper, a middle and a lower position. A proband then exerted forces onto the arm brace by pushing its arm up and down. The interaction torque was measured using the torque sensor, all four force sensors in both cuffs and only two force sensors in the front cuff. Exemplary for an upward and downward force exertion of the proband the different resulting human-robot interaction torques are depicted in Fig. 3, while the arm brace was fixed in an upper position. In the depicted case, good detection of the human-robot interaction torque using the sensors in both arm cuffs can be observed. However, if we only demand a good qualitative detection of the current desired motion of the human arm rather than the measurement of the precise value of the corresponding interaction torque, using the two sensors in the front cuff is sufficient. This can be seen if we normalize the signals with respect to their maximum absolute value, that is

$$\bar{\tau}_{\text{he}}(t) = \frac{\tau_{\text{he}}(t)}{\max_t (|\tau_{\text{he}}(t)|)} \quad , \quad (2)$$

where $\bar{v}_{he}(t)$ denotes the normalized signal. The normalized signals of the front ring sensors and the torque sensor are depicted in Fig. 4 and show good correlation. Note that the signals of the upward and downward motion were normalized separately.

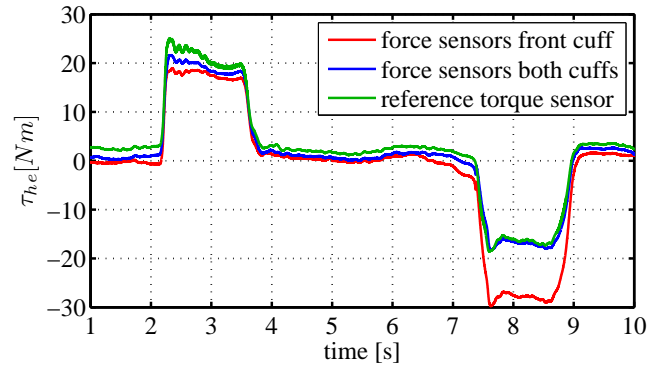


Fig. 3 Human-robot interaction torque for an upward and downward force exertion of the proband

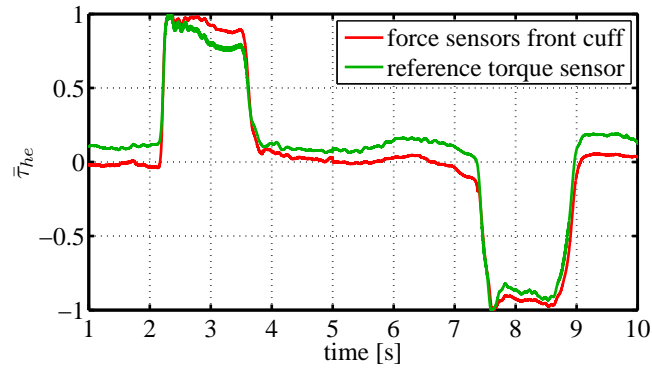


Fig. 4 Normalized human-robot interaction torques measured by the sensors in the front arm cuff and by the torque sensor

In the second mode, that is if active force support is required, an additional command signal by the user is necessary, as mentioned above. For this purpose, we propose a sensor glove which provides an intuitive user interface.

3 Control Concept

Two high-level control concepts based on the presented sensor concept are proposed, based on impedance and on admittance control, respectively. Both concepts are (in the linear case) equivalent, however, differences arise in practical implementation. While in admittance control kinematic values are calculated for given forces, in impedance control the inverse calculation is done. The relation between the kinematic and kinetic values is typically given by a second order system, that is both approaches simulate a virtual system in each joint with dynamic behavior

$$J_v \ddot{\phi}_d + D_v \dot{\phi}_d + C_v \phi_d = \tau_{he} - \tau_{hc} =: \tau_h \quad . \quad (3)$$

The angle ϕ_d denotes the desired elbow joint position, as indicated in Fig 2. The impedance parameters J_v , D_v and C_v are the desired moment of inertia, damping and stiffness, respectively, for the virtual system, τ_{he} denotes the human-robot interaction torque around the joint and τ_{hc} represents the torque commanded by the user, e.g. by using a sensor glove. The resulting net torque τ_h denotes the total desired torque commanded by the user.

3.1 Admittance Control Approach

Based on (3) the proposed admittance control approach calculates a set-point angular velocity for the actuated joints for a measured interaction torque. The angular velocity value is then passed to the low-level motor controller, which carries out velocity control. Velocity control is used as it shows better performance in human-robot cooperation [2], in contrast to position control. Fig. 5(a) depicts the control structure of the admittance control approach. The admittance transfer function can be calculated from (3) as

$$Y(s) = \frac{\mathcal{L}(\dot{\phi}_d)}{\mathcal{L}(\tau_h)} = \frac{s}{J_v s^2 + D_v s + C_v} \quad , \quad (4)$$

with s denoting the Laplace variable and $\mathcal{L}(\cdot)$ the Laplace transformation. As no static force is desired, stiffness is set to zero, that is $C_v = 0$. It is desirable to set the dynamic parameters for inertia and damping as small as possible in order to achieve high dynamic movements, however, there exist limits in terms of measurement noise and stability. The latter is discussed below. Regarding noise reduction observe that for $C_v = 0$, (4) becomes a first order low-pass filter with cutoff frequency $\omega_c = \frac{D_v}{J_v}$ and static gain $\frac{1}{D_v}$, that is both damping and inertia must be chosen large enough to suppress noise.

Collision of the robot arm with the end positions is prevented by increasing the damping parameter according to

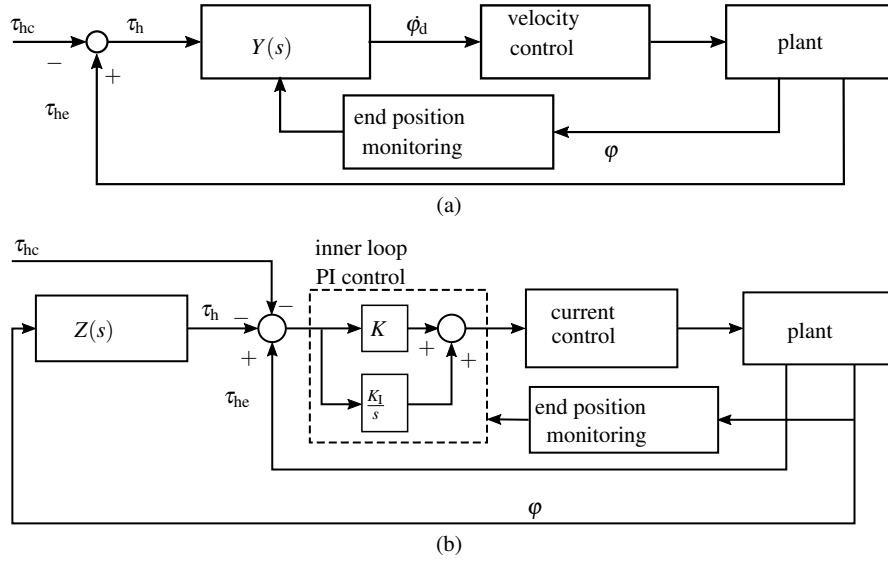


Fig. 5 Structure of (a) the admittance control approach and (b) of the control approach based on impedance control with inner torque control loop

$$D_v = \begin{cases} D_{v_n} & \text{for } \phi_{\min} + \gamma < \phi < \phi_{\max} - \gamma \\ D_{v_{\max}} \left(1 + \frac{(\phi_{\min} - \phi)}{\gamma}\right)^5 + D_{v_n} & \text{for } \phi \leq \phi_{\min} + \gamma \\ D_{v_{\max}} \left(1 - \frac{(\phi_{\max} - \phi)}{\gamma}\right)^5 + D_{v_n} & \text{for } \phi \geq \phi_{\max} - \gamma \end{cases} \quad (5)$$

with elbow angular position ϕ_d , tuning parameters γ specifying the end zone in which damping increases, D_{v_n} the nominal and $D_{v_{\max}}$ the maximum damping value. Note that damping is only increased if the user's desired movement, indicated by the sign of the interaction torque, is towards the end position.

3.2 Impedance Control Approach

In contrast to the admittance control approach presented above, the impedance controller calculates a set-point motor torque, which is fed into the low-level torque controller of the motor controller. Fig. 5(b) depicts the structure of the controller. From (3), the impedance transfer function follows as

$$Z(s) = \frac{\mathcal{L}(\tau_h)}{\mathcal{L}(\phi)} = J_v s^2 + D_v s + C_v \quad . \quad (6)$$

To achieve high dynamics the impedance parameters are set to zero such that (6) reduces to $\tau_h = 0$, that is the impedance controller degenerates to the special case of a zero torque controller. Even so, it is referred to as impedance controller in the following. To compensate for friction and inertia of the actuator the measured torque is fed back into an inner-loop proportional-integral controller. Note that despite setting the impedance parameters to zero, the system does, of course, not simulate a dynamic behavior corresponding to zero inertia and zero damping. Consider the simplified dynamics of the geared motor joint, that is

$$J\ddot{\phi} + B\dot{\phi} + H(\eta) = \tau_h + \tau_m \quad , \quad (7)$$

with inertia J and viscous damping factor B . According to the LuGre model [1], functional H accounts for other friction components, such as hysteresis and the Stribeck effect, and is described by another differential equation with internal state η . Variable τ_m denotes the motor output torque, τ_{hc} is set to zero. Assuming a proportional controller with gain K , it holds $\tau_m = K\tau_h$, hence

$$\frac{J}{1+K}\ddot{\phi} + \frac{B}{1+K}\dot{\phi} + \frac{H(\eta)}{1+K} = \tau_h \quad . \quad (8)$$

The inertia and damping felt by the user is hence reduced by the factor $1 + K$. Collision with the end positions could be prevented by increasing the damping parameter D_v , analogous to the admittance approach. Then, however, online differentiation of the position signal is required, as follows from (6). Alternatively, adjusting the inner-loop PI controller by reducing the proportional gain and setting the integral gain to zero is proposed such that the motor dynamics are scaled according to (8) and the user experiences higher resistance in terms of damping and inertia. For the minimal end position, K is adjusted according to a polynomial function of order four with constraints $K(\varphi_{\min} + \frac{\gamma}{2} < \varphi < \varphi_{\min} + \gamma) = 0$, $K(\varphi = \varphi_{\min}) = -125$ and $K(\varphi = \varphi_{\min} - \gamma) = -500$. Similarly, the gain is adjusted when approaching the maximal end position. Anti-windup is used to account for the limitation of the motor current, but not depicted in Fig. 5(b).

3.3 On the Stability of the Control Approaches

Various researchers discussed stability of impedance-based controllers in human-robot contact tasks, [16] gives a good overview. In [8] stability of a position based-impedance control was compared to a force-based impedance control in terms of the influence of stiffness and damping, the influence of inertia was outside of the scope. Similarly, in [20] stability of an impedance controller in human-robot cooperation was investigated. However, influence of inertia and the case with an inner loop controller, as we use in this paper, were not covered.

Stability of the presented impedance-based controllers strongly depends on the human user, who himself is stabilizing the control loop by means of his own impedance

characteristics. To achieve stability of the presented admittance and impedance controllers tuning of the impedance parameters and the inner loop proportional gain, respectively, is necessary. To show the influence of these parameters and the human impedance on stability of the given approaches, we derive a linear dynamic model of the control chain. Fig. 6 depicts the closed loop of the plant and both the admittance and impedance controller. The human skin muscle model of the arm is modeled as

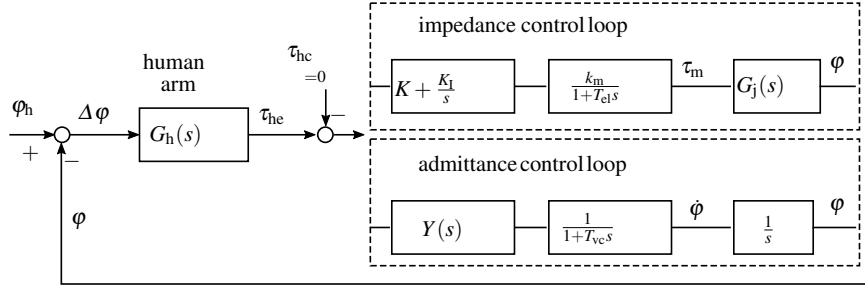


Fig. 6 Linear model of the closed loops of the impedance and admittance controllers

a second-order spring-mass-damper system, similar to the approach in [20], that is

$$G_h(s) = \frac{\mathcal{L}(\tau_{he})}{\mathcal{L}(\Delta\varphi)} = (l_b^2 + l_f^2) (M_h s^2 + D_h s + C_h), \quad (9)$$

with human impedance parameters set to $M_h = 0.015$ kg, $D_h = 25$ Nsm $^{-1}$ and $C_h = 625$ Nm $^{-1}$, according to [10], and deviation between angular position of the human and the exoskeleton arm $\Delta\varphi = \varphi_h - \varphi$. Note that the impedance parameters need to be scaled by $l_b^2 + l_f^2$ as they hold for linear deviations Δx_f and Δx_b and forces F_f and F_b acting on the front and back arm cuff, respectively, that is

$$M_h \Delta \ddot{x}_{b,f} + D_h \Delta \dot{x}_{b,f} + C_h \Delta x_{b,f} = F_{b,f}, \quad (10)$$

with $\Delta x_{b,f} = l_{b,f} \sin(\Delta\varphi) \approx l_{b,f} \Delta\varphi$, for small $\Delta\varphi$.

The current and velocity control loops are modeled as first order lags, with time constants determined in measurements as $T_{el} = 0.001$ s and $T_{vc} = 0.01$ s, respectively. The torque constant of the motor is $k_m = 7.05$ NmA $^{-1}$, taking into account the gear ratio. For the dynamics of the joint, viscous damping is assumed, that is

$$G_j(s) = \frac{\mathcal{L}(\varphi)}{\mathcal{L}(\tau_m)} = \frac{1}{J_m s^2 + D_m s}, \quad (11)$$

with viscous damping coefficient $D_m = 4.5$ Nm s rad $^{-1}$ and the inertia of the motor and forearm construction calculated as $J_m = 3$ kgm 2 under consideration of the gear ratio.

From Fig. 6 the open loop transfer function of the impedance control loop then calculates as

$$\begin{aligned}
G_{0I}(s) &= \frac{\mathcal{L}(\varphi)}{\mathcal{L}(\Delta\varphi)} \\
&= \frac{(I_b^2 + I_f^2)k_m(KM_h s^3 + (KD_h + K_I M_h)s^2 + (KC_h + K_I D_h)s + K_I C_h)}{(J_m T_{el} + D_m T_{el} T_h)s^4 + (D_m T_{el} + J_m)s^3 + D_m s^2}.
\end{aligned} \tag{12}$$

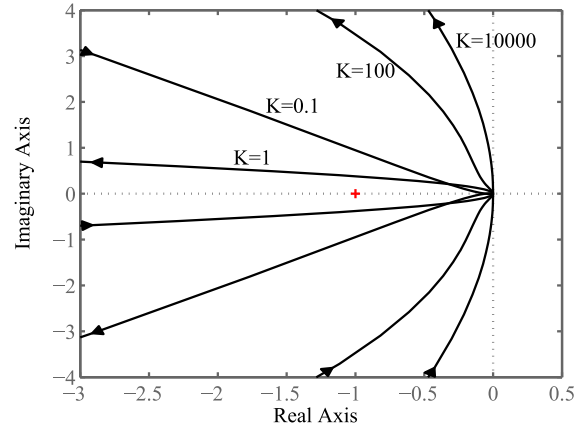
For the given parameter values (12) has two stable poles and two poles in the origin of the complex plane. Stability strongly depends firstly on the human stiffness M_h and secondly on the proportional gain K and the virtual inertia J_v for the impedance and admittance approach, respectively.

Fig. 7(a) gives the Nyquist plots of (12) for varying proportional gains and given human stiffness. Obviously, decreasing the gain leads to instability, in the given case this occurs at $K = 0.1$ (observe the arrows indicating the direction of increase of frequency), according to the Nyquist criterion. Note that due to a double integrator in the open loop the locus needs to be closed at infinity to check for stability. Similarly, in Fig. 7(b) the Nyquist plots are given for the same gains but a higher human stiffness. In this case, $K = 100$ already leads to instability of the closed loop. Increasing K stabilizes the loop in case of a stiff environment, however, there exist upper bounds. Firstly, oscillations increase due to measurement noise, and secondly, the control loop becomes unstable in presence of time delays, e.g. due to communication delays. In Fig. 7(c) the Nyquist plot of (12) is given, for $K = 250$ and $C_h = 625 \text{ Nm}^{-1}$. An output time delay of 1 ms is incorporated, representing possible communication delays. The depicted case is stable, however, increasing K by the factor of approx. 2 will give an instable closed loop.

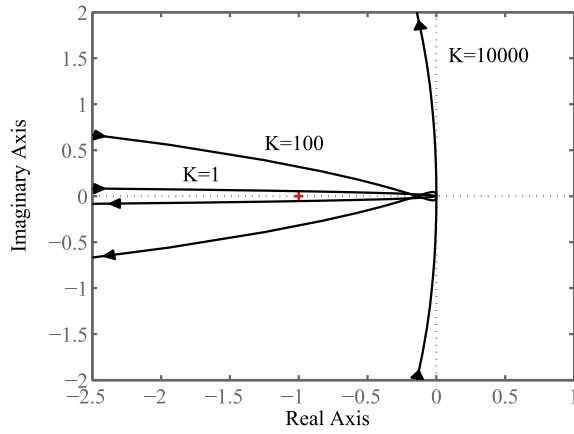
Similar results for stability analysis of the admittance controller are obtained, but not plotted here. Decreasing J_v leads to higher dynamics and a stable loop in presence of stiff environments with the same constraints applying in terms of time delays.

4 Evaluation

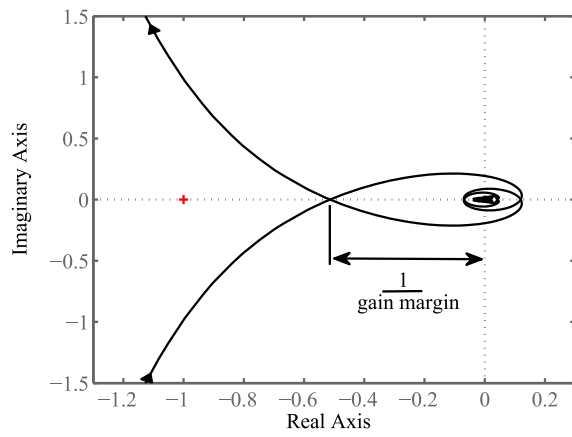
The proposed controllers in combination with the two force sensors in the front arm cuff were tested on the test stand depicted in Fig. 1. The elbow joint is actuated by a brushless DC motor (Maxon EC 90 flat) in conjunction with a Harmonic Drive gear (type HFUC-20-100-2A) with a reduction ratio of 100 : 1. The nominal output torque of the drive section is 44 Nm at a nominal angular velocity of 26 rpm. The used motor controller (Maxon EPOS 70/10) can be configured for position, velocity or current control. An incremental rotary encoder is used for motor low level control and for end position monitoring. In the front cuff of the arm brace two resistive force sensors (Tekscan FlexiForce A201) are used to detect the human-robot interaction torque, according to Section 2. The used sensors have been shown to be suitable for control applications [9]. A one-axis torque sensor in the elbow joint is used as reference signal, it is based on strain gauges and able to detect torques up to 30 Nm. Its signal is compensated for the weight of the forearm construction. The controllers are realized in MATLAB/SIMULINK in conjunction with a rapid prototyping system



(a)



(b)



(c)

Fig. 7 Nyquist plots of the impedance control open loop for various proportional gains K and fixed human stiffness (a) $C_h = 625 \text{ Nm}^{-1}$ and (b) $C_h = 62500 \text{ Nm}^{-1}$ and (c) in presence of an output time delay of 1 ms

(dSPACE DS1103), providing serial, digital and analogue interfaces. The real-time application is running on 10 kHz, however, an update of the joint's angular position is provided by the serial communication interface every 4 ms only, that is at 250 Hz. The user activates the device using a dead-man switch in the right hand. The human command torque τ_{hc} is set to zero, that is no sensor glove is used. The parameters of the admittance controller were chosen as $J_v = 0.1 \text{ kgm}^2$ and $D_v = 0.1 \text{ Nms}$, the proportional gain of the impedance controller was set to $K = 10000$, the integral gain to $K_I = 1$. These parameters revealed good dynamic behavior while maintaining stability and noise suppression of the force signal.

Both the admittance and impedance control approach showed good results in terms of realizing a movement of the elbow joint according to the user's intention. In Fig. 8 the motor position and the interaction torque for an oscillating movement using impedance control are given. At the end of the plotted section the proband moves

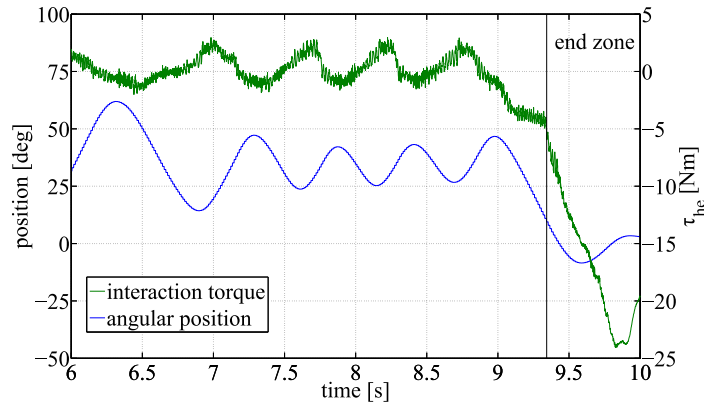


Fig. 8 Interaction torque and measured angular position of the arm for an oscillating movement

towards the minimal end position and enters the end zone at approx 9.4 s, as indicated by the vertical line. The proportional gain is then reduced according to (8) and the user needs to exert a significant higher torque, which gives an intuitive feedback that the end position is reached. The arm stops slightly after the defined end position, which is acceptable, as φ_{\min} is defined before the hardware end position. Hence, it is not even necessary to switch to velocity control mode to stop the motor at the end position. Compared to the impedance controller, the admittance controller was felt by various probands to be less dynamic than the impedance control approach. For objective comparison of both approaches, sinusoidal input force signals were simulated while no user was wearing the exoskeleton arm. The phase delays of the corresponding measured position were determined for various frequencies of the force signals, see Fig. 9. Significant higher phase delays using the admittance controller can be observed compared to the impedance controller, which correlates with the subjective feeling reported by the probands.

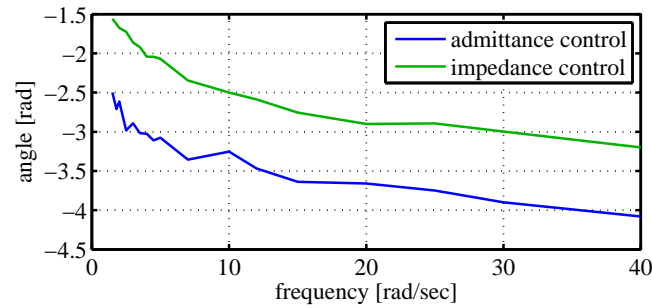


Fig. 9 Measured phase plot of the admittance and impedance control loops for interaction torque as input signal and position response

5 Discussion and Conclusion

In this paper, a concept for an exoskeleton for assistance in MHL tasks in industry was presented. In contrast to existing systems, the presented approach focuses on the special requirements in industry and MHL tasks regarding cost, weight and an intuitive control interface. No bio-signals but light and economic force sensor were proposed for the forearm to allow easy and fast set-up of the system. It was shown that two sensors in the front cuff of the arm brace only can be used to control the elbow joint, while still providing a revolute joint for pronation and supination of the forearm. In measurements they were shown to provide good detection of the human-robot interaction torque, a torque sensor in the elbow joint was used as reference signal. An impedance and admittance control approach based on the force sensor concept were compared, which allow free movement of the user while wearing the robot and not handling any load. Force support mode is incorporated by using an external user command signal, e.g. by means of a sensor glove. This approach allows the user to handle loads directly using his hands without need to handle a grip. For both approaches a linear model of the closed control chain was derived to identify the influence of the control parameters, human impedance characteristics and possible time delays onto stability. Calculations revealed that even for a significant higher stiffness than the standard human stiffness value, stability can be achieved by appropriate tuning of the controllers.

A test stand with an actuated elbow joint was built up to evaluate the proposed concept. Both control approaches revealed good performance, while the impedance approach showed to be superior. Proband reported it to behave more dynamically, which was confirmed in measurements.

Future work targets at building up a lightweight arm construction based on the presented control and sensor concept, comprising of two actuated joints and a torque sensor in the shoulder joint.

Acknowledgements This work was supported as a Fraunhofer Master Project.

References

1. Canudas de Wit, C., Olsson, H., Astrom, K.J., Lischinsky, P.: A new model for control of systems with friction. *IEEE Transactions on Automatic Control* **40**(3), 419–425 (1995)
2. Duchaine, V., Gosselin, C.M.: General model of human-robot cooperation using a novel velocity based variable impedance control. In: 2nd Joint EuroHaptics Conf. and Symp. on Haptic Interfaces for Virtual Environment and Teleoperator Systems (WHC), pp. 446–451 (2007)
3. Gunasekara, J., Gopura, R., Jayawardane, T., Lalitharathne, S.: Control methodologies for upper limb exoskeleton robots. In: IEEE/SICE International Symposium on System Integration, pp. 19–24 (2012)
4. Hayashi, T., Kawamoto, H., Sankai, Y.: Control method of robot suit HAL working as operator's muscle using biological and dynamical information. In: IEEE/RSJ International Conference on Intelligent Robots and Systems, pp. 3063–3068 (2005)
5. Kazerooni, H., Steger, R.: The berkeley lower extremity exoskeleton. *Journal of Dynamic Systems, Measurement, and Control* **128**(1), 14 (2006)
6. Khan, A.M., Yun, D.w., Ali, M.A., Han, J., Shin, K., Han, C.: Adaptive impedance control for upper limb assist exoskeleton. In: IEEE International Conference on Robotics and Automation (ICRA), pp. 4359–4366 (2015)
7. Kiguchi, K., Hayashi, Y.: An EMG-based control for an upper-limb power-assist exoskeleton robot. *IEEE transactions on systems, man, and cybernetics. Part B, Cybernetics : a publication of the IEEE Systems, Man, and Cybernetics Society* pp. 1064–1071 (2012)
8. Lawrence, D.A.: Impedance control stability properties in common implementations. In: IEEE International Conference on Robotics and Automation, pp. 1185–1190 (1988)
9. Lebosse, C., Renaud, P., Bayle, B., Mathelin, M.d.: Modeling and evaluation of low-cost force sensors. *IEEE Transactions on Robotics* **27**(4), 815–822 (2011)
10. Minyong, P., Mouri, K., Kitagawa, H., Miyoshi, T., Terashima, K.: Hybrid impedance and force control for massage system by using humanoid multi-fingered robot hand. In: IEEE International Conference on Systems, Man and Cybernetics, pp. 3021–3026 (2007)
11. Muramatsu, Y., Umehara, H., Kobayashi, H.: Improvement and quantitative performance estimation of the back support muscle suit. In: Annual International Conference of the IEEE Engineering in Medicine and Biology Society, pp. 2844–2849 (2013)
12. Nagarajan, U., Aguirre-Ollinger, G., Goswami, A.: Integral admittance shaping for exoskeleton control. In: IEEE Int. Conf. on Robotics and Automation (ICRA), pp. 5641–5648 (2015)
13. Neville Hogan: Impedance control: An approach to manipulation. In: 1984 American Control Conference, pp. 304–313 (1984)
14. Otten, B., Stelzer, P., Weidner, R., Argubi-Wollesen, A., Wulfsberg, J.: A novel concept for wearable, modular and soft support systems used in industrial environments. In: Hawaii International Conference on System Sciences 2016 (2016)
15. Perry, J.C., Rosen, J., Burns, S.: Upper-limb powered exoskeleton design. *IEEE/ASME Transactions on Mechatronics* **12**(4), 408–417 (2007)
16. Pons, J.L.: *Wearable robots: Biomechatronic exoskeletons*. Wiley, Hoboken, N.J. (2008)
17. Schneider E., Irastorza X.: Osh in figures: work-related musculoskeletal disorders in the eu - facts and figures (2010). URL <https://osha.europa.eu/en/publications/reports/TERO09009ENC>
18. Singh, R.M., Chatterji, S., Kumar, A.: A review on surface EMG based control schemes of exoskeleton robot in stroke rehabilitation. In: International Conference on Machine Intelligence and Research Advancement (ICMIRA), pp. 310–315 (2013)
19. Stelzer, P., Kraus, W., Pott, A.: Sensor glove for an intuitive human-machine interface for exoskeletons as manual load handling assistance. In: International Symposium on Robotics 2016 (2016). Forthcoming
20. Tsumugiwa, T., Yokogawa, R., Yoshida, K.: Stability analysis for impedance control of robot for human-robot cooperative task system. In: IEEE/RSJ International Conference on Intelligent Robots and Systems (IROS), pp. 3883–3888 (2004)
21. Vukobratović, M.: How to control robots interacting with dynamic environment. *Journal of Intelligent and Robotic Systems* **19**(2), 119–152 (1997)